Water SA 48(3) 295–303 / Jul 2022
https://doi.org/10.17159/wsa/2022.v48.i3.3909

Research paper

Optimization, characterization and adsorption properties of natural calcite for toxic As(III) removal from aqueous solutions

Khizar Hussain Shah[1], Muhammad Fahad[2,3], Zahid Ali Ghazi[4], Sajjad Ali[5], Asim Shahzad[6] and Salah Ud Din[7]

[1]Department of Chemistry, COMSATS University Islamabad, Abbottabad Campus, University Road 22060, Abbottabad, Pakistan
[2]Department of Electrical and Computer Engineering, COMSATS University Islamabad, Abbottabad Campus, University Road 22060, Abbottabad, Pakistan
[3]AlchLight LLC, 1999 Lake Avenue, Rochester, New York 14650, United States of America
[4]National Centre of Excellence in Physical Chemistry, University of Peshawar, 25120 Peshawar, Pakistan
[5]Materials Research Laboratory, Department of Physics, University of Peshawar, 25120 Peshawar, Pakistan
[6]School of Geosciences and Info-Physics, Geosciences Building, Central South University, Changsha 410083, China
[7]Department of Chemistry, University of Azad Jammu and Kashmir, Muzaffarabad 13100, Pakistan

The potential of natural (N) and magnetized (M) forms of different rocks (calcite and dolomite) and clays (bentonite, kaolinite, and hematite) were evaluated for the removal of As(III) from aqueous solutions, in order to optimize and scrutinize the most suitable adsorbent. The order observed for efficiency of As(III) removal was N-calcite > N-dolomite > M-calcite > M-dolomite > N-bentonite > M-bentonite > M-kaolinite > N-kaolinite > M-hematite > N-hematite. On the basis of this analysis, natural calcite was further selected for in-depth analysis of various adsorption parameters such as time, pH, temperature, dosage, and concentration of As(III) ions. An excellent adsorption capacity of 19.05 mg·g^{-1} was displayed by calcite for As(III), which was significantly higher than that previously reported for other studies. The characterization of adsorbent calcite was performed by various analytical techniques: XRD, XRF, FTIR, SEM-EDS, TG/DTA and PZC. The kinetic investigation revealed that the adsorbent successfully removed over 98% of As(III) from aqueous solution after 160 minutes of equilibration time. The adsorption data was well fitted to the Freundlich isotherm model and fairly described by the pseudo-second-order mechanism. The mean energy of adsorption (*E*) determined from the Dubinin-Radushkevich (D-R) model was less than 8 kJ·mol^{-1}, which indicates a physical adsorption process. The calculated thermodynamic parameters revealed that the adsorption of As(III) by calcite is endothermic, favourable and spontaneous.

CORRESPONDENCE
Muhammad Fahad

EMAIL
drmuhammadfahad@gmail.com

DATES
Received: 3 June 2021
Accepted: 22 June 2022

KEYWORDS
calcite
characterization
separation
kinetic studies
physisorption
As(III) removal

COPYRIGHT
© The Author(s)
Published under a Creative Commons Attribution 4.0 International Licence (CC BY 4.0)

INTRODUCTION

Arsenic (As) is considered one of the extremely toxic heavy metals in drinking water and industrial wastewaters. High and prolonged exposure to As could lead to many genetic complications, arsenicosis and other dangerous diseases in humans and many other organisms and. Also, the presence of As severely impacts the quality of water, air and soil. Therefore, the World Health Organization (WHO) and United States Environmental Protection Agency (USEPA) have recommended a maximum permissible limit of As in drinking water of 10 μg·L^{-1} (Hernandez et al., 2018; Jeon et al., 2018). In the current scenario, many areas of the world are facing a major environmental problem due to As contamination of water bodies (Hao et al., 2018). Many countries in the world are badly affected by As pollution, with consumption of As-rich drinking water and food (Aredes et al., 2012; Ramos et al., 2009). In Pakistan, particularly in the highly contaminated cities of Punjab and Sindh provinces, the As level has been observed to exceed the permissible limit (>50 μg·L^{-1}) which is an alarming and risky situation for the communities living in these regions (Sanjrani et al., 2017).

In the aquatic system, As mainly occurs in two soluble stable oxidation forms, trivalent arsenite As(III) and pentavalent arsenate As(V) (Aredes et al., 2012; Liu et al., 2015). In comparison to As(V), As(III) is considered to be a more injurious, mutagenic, and carcinogenic species in nature (Amer et al., 2018). Therefore, it is necessary to remove both forms of arsenic to improve water quality and avoid degradation of water resources. In the current study, our main focus was to investigate an economically viable potential adsorbent for the removal of As(III), because of its acute toxicity and the greater difficulty in removing it from water solutions than As(V). To remove As from aqueous solution and attain a concentration below the permissible limit, several technologies have been adopted, including electrochemical treatment, membrane processes, photocatalysis, precipitation, ion exchange and adsorption. Among all these techniques, adsorption has is considered to be the most economical, simple, and easy to operate, as in this technique the regeneration of adsorbent and adsorbate is possible (Lin et al., 2018; Sadri et al., 2018). Since the performance of the adsorption technique is highly dependent on the quality and cost-effectiveness of the adsorbent material, the selection of a suitable adsorbent is an important decision.

Recently, the application of natural clays and their chemically modified forms as adsorbents has received a lot of attention from researchers, due to the good adsorption capability of clays, stripping

toxins from aqueous solutions in a short time (Alshameria et al., 2018; Gan et al., 2019; Momina et al., 2019). However, various publications also report that the modifications to natural clays decrease the overall adsorption potential due to the partial occupation of adsorption sites at the surface by chemicals involved in modification (Siddiqui et al., 2017; Vilardi et al., 2018; Yu et al., 2018). Moreover, modification of natural clays can increase the synthesis cost, result in difficulties in separating the adsorbent from water, and also results in the production of huge amount of sludge after adsorption.

The surface modification of natural clays with magnetic oxide nanoparticles (Fe_3O_4) is considered very promising because of several advantages, such as ease of recovery, green synthesis, cost-effectiveness and good handling through successive surface functionalization. The separation of adsorbent after the adsorption process using an external magnetic field is highly feasible, to avoid adsorbent dispersion in the aqueous phase. This makes magnetized clays an excellent and novel candidate for combining good adsorption characteristics with easy phase separation.

In the present investigation, natural and magnetic forms of different carbonate rocks (calcite, dolomite and hematite) and clays (bentonite and kaolinite) were tested for the removal of As(III), to assess their adsorption capabilities in order to select the most appropriate and promising adsorbent. Based on preliminary adsorption experiments, natural calcite was chosen as the best option and was selected for further detailed studies, including characterization and adsorption potential under different experimental conditions for temperature, pH, time, concentration, and adsorbent dosage. It is necessary to mention that the current study represents the first attempt to compare the As(III) adsorption potential of natural calcite with other popular clay and rock-based adsorbents in native and magnetic forms. This paper is also offers useful information for the application of natural Pakistani calcite in the environmental engineering field and provides recommendations for utilizing this adsorbent in future water treatment research.

MATERIALS AND METHODS

Chemicals and reagents

All chemicals used were of analytical grade and high purity, and were used without any further purification. Hydrochloric acid (HCl), nitric acid (HNO_3), sodium chloride (NaCl), sodium hydroxide (NaOH) and arsenic trioxide (As_2O_3) were obtained from Daejung Company (South Korea). Different adsorbents in natural forms – calcite, dolomite, hematite, bentonite and kaolinite –were collected as a raw material from Khyber Pakthunkhawa (KPK) province, northern Pakistan. The working and standard solutions of As(III) were synthesized with triply de-ionized water during the adsorption experiments. A stock solution of As(III) (1 000 mg·L^{-1}) was prepared by dissolving 1.32 g As_2O_3 in 25 mL of NaOH (1M) solution. The mixture was then diluted to 100 mL with de-ionized water. Then 50 mL of HCl (1M) solution was added until the solution became neutral. The neutral solution was transferred into a 1 000 mL volumetric flask and made up to the mark with de-ionized water. The standard As(III) solutions (10–2 500 µg·L^{-1}) were prepared by appropriate dilution of stock solution using de-ionized water. The pH of solutions was adjusted by 0.01 M sodium hydroxide and hydrochloric acid solutions.

Preparation of adsorbents

For adsorbent preparation, first natural adsorbents (calcite, dolomite, bentonite and kaolinite) were washed with highly pure acetone for complete removal of dust particles and other impurities. The adsorbents were then powdered by metal file and crushed in a mortar to further reduce the particle size. Fine powdered adsorbent was then washed with deionized water and dried at 102°C for 24 h. For magnetization of adsorbents, first magnetic oxide (Fe_3O_4) was prepared by reacting $FeSO_4{\cdot}7H_2O$ (2.1 g) and $FeCl_3{\cdot}6H_2O$ (3.1 g), each dissolved in 80 mL of deionized water under an inert atmosphere. The mixed solution was heated at 80°C and 10 mL NH_4OH (25%) was added dropwise until the appearance of black precipitate. The natural adsorbents (10 g) were then mixed with reaction mixture separately at 80°C for 1 h in order to grow magnetic oxide nanoparticles on the surface of adsorbents. After settling the suspension, the magnetized adsorbents were washed, dried and separated for further investigation (Anneerselvam et al., 2011; Shah et al., 2018).

Initial screening of adsorbents for removal of As(III)

In preliminary investigations, five different types of natural and widely available adsorbent (calcite, dolomite, bentonite, kaolinite and hematite) in native and magnetic forms were selected to screen out the best adsorbent for As(III) removal. The batch adsorption technique was used, setting the experimental conditions viz. dosage as 0.02 g in 40 mL of 1 mg·L^{-1} As(III) solution, at a temperature of 298 K, pH of 6.5, contact time 240 min and 200 r·min^{-1} agitation speed. The basis for selecting the best adsorbent was the per cent removal of As(III) from aqueous solution.

Characterization

In order to examine the surface morphology and study the chemical composition of natural calcite adsorbent, a scanning electron microscope (JEOL JSM5910 SEM-EDS, Japan) coupled with energy dispersive X-ray spectroscopy (EDS INCA200, Oxford Instruments, UK) was used. For phase identification and crystal structure, X-ray diffraction patterns were obtained using Bruker D8 advance X-ray diffractometer with Cu Kα radiation (λ = 0.1542 nm) operating at 40 kV and 40 mA, whereas the determination of the chemical composition of the adsorbent in powdered form was performed using energy dispersive X-ray fluorescence spectrometry (XRF). Thermal stabilities were explored using simultaneous thermo-gravimetric and differential analysis (TG/DTA) machine (PerkinElmer, USA) in a N_2-gas dynamic atmosphere (20 mL·min^{-1}) at a heating rate of 10°C·min^{-1} and temperature range 30–1 200°C. To assess the presence of different functional groups and reaction sites in the adsorbent, Fourier transform infra-red (FT-IR) analysis was performed in the range of 4 000–400 cm^{-1} using a FTIR spectrophotometer (Shimadzu 8202PC, Kyoto Japan). The point of zero charge (pH_{pzc}) of calcite adsorbent was determined by the well-known salt addition method (Shah et al., 2018). To each flask of a series of 50 mL conical flasks, 0.1 g of adsorbent was poured into 40 mL solution of 0.01 M $NaNO_3$ background electrolyte solution. The pH of solution was maintained by using standardized 0.01 M HNO_3 and 0.01 M NaOH to obtain a required range of pH values (2–11). The pH values of the suspension in each flask were recorded as initial pH (pH_i) using pH meter model BOECO BT-600 (Germany). After closing the conical flasks, the suspension were shaken for about 4 h using a thermostatic shaker bath at 200 r·min^{-1}. The final pH (pH_f) values of the suspension in each flask were measured using a pH meter. The difference between pH_i and pH_f (ΔpH) was plotted against pH_i; the point of intersection equals the PZC of the adsorbent.

Adsorption studies

The adsorption experiments were performed in a batch adsorption system. To conduct the kinetic investigation, 0.02 g of

adsorbent was mixed with 100 mL of As(III) solution (1 mg·L^{-1}) at different temperatures (298–333K). After regular time intervals (15–180 min), 1 mL amounts of the suspensions were taken and subjected to As(III) determination. To examine the influence of pH, 0.02 g of adsorbent was poured into a 40 mL solution of As(III) having a concentration of 1 mg·L^{-1} in the range of pH 2–12 at 298 K. Likewise, to observe the effect of dosage on adsorption, adsorbent dosages were varied from 5 to 40 mg using As(III) concentration (1 mg·L^{-1}) for 160 min. To examine the influence of temperature on adsorption, 0.02 g of adsorbent was contacted with 2–10 mg·L^{-1} of As(III) solution (40 mL) at an initial pH of 7. The suspensions were agitated in a thermostatic shaker bath for 160 min at 200 r·min^{-1} in the temperature range of 298–333 K. The pH of the solution was maintained using hydrochloric acid or sodium hydroxide solutions. The residual As(III) concentration in solution was determined by the method given in literature using a UV-Vis spectrophotometer (UV-759S, Jinghua, China) (Cherian and Narayana, 2005). All the adsorption experiments were performed in triplicate and results obtained were the average of three concordant readings.

The percentage removal (%) of adsorbent and maximum adsorption capacity (X) per unit mass, respectively, were calculated using the following equations:

$$\% \text{ Removal efficiency} = \frac{C_i\text{-}C_e}{C_i} \times 100 \quad (1)$$

$$X = \frac{V \cdot (C_i - C_e)}{1000\,\text{m}} \quad (2)$$

where C_i is initial concentration (mg·L^{-1}) and C_e is equilibrium concentration (mg·L^{-1}) of As(III) solution. X is the amount of As(III) ion adsorbed (mg·g^{-1}), m is the weight (g) of adsorbent while V is the volume of solution (mL).

RESULTS AND DISCUSSION

Initial screening of adsorbents for removal of As(III)

The adsorbents selected for preliminary investigation, viz. calcite, dolomite, bentonite, kaolinite and hematite in native and magnetic forms, were applied in a batch adsorption technique for As(III) removal. The results are shown in Fig. 1, which indicates the performance of these adsorbents in terms of per cent removal of As(III). It is clear from Fig. 1 that natural calcite exhibited the best efficiency for As(III) removal compared to its counterparts. Thus, natural calcite adsorbent was selected for further detailed investigation, characterization, and adsorption studies for As(III) removal under different experimental conditions for pH, contact time, temperature, dosage amount and initial metal ion concentration.

XRD phase analysis

The XRD patterns of calcite adsorbent are shown in Fig. 2a. It can be clearly seen that most of the XRD diffraction peaks and their corresponding intensities match the calcite phase, indicating its dominance in the studied sample. The most prominent peaks for the calcite phase were observed at 2θ = 29.47° and 47.6°, corresponding to d-spacing of 3.03 and 1.91 Å and hkl values of 104 and 024, respectively. A few low intensity peaks were also observed indicating the presence of quartz (2θ = 20.8°, 26.6° and 50.2°) and dolomite as minor phases (2θ = 60.7°) (Fahad et al., 2016; Fahad et al., 2018).

XRF chemical analysis

The chemical composition of calcite adsorbent, determined by XRF, is presented in Table 1. The table shows that calcite adsorbent contains CaO (45.7%) in the highest amount, followed by SiO_2 (~18%) indicating their presence as major elements; however, traces of Na_2O, Al_2O_3, MgO, K_2O and Fe_2O_3 were also detected in the sample.

TG/DTA analysis

TG/DTA characterizations were used for studying thermal stabilities and quantitative analysis of calcite adsorbent (Fig. 2b). The net weight loss of adsorbent was noted to be 34.6 wt.% following the temperature range 25–1 200°C. The TG curve revealed two significant weight loss regions. The weight loss from 200–600°C temperature region was found to be not more than 0.60 wt.%. Within the same region at about < 200°C, the observed weight loss was 0.15 wt.% due to the dehydration of the sample. The most rapid weight loss was observed in the 700–800°C temperature range which is indicative of calcite decomposition ($CaCO_{3(s)} \rightarrow CaO_{(s)} + CO_{2(g)}$) (Fahad and Iqbal, 2014).

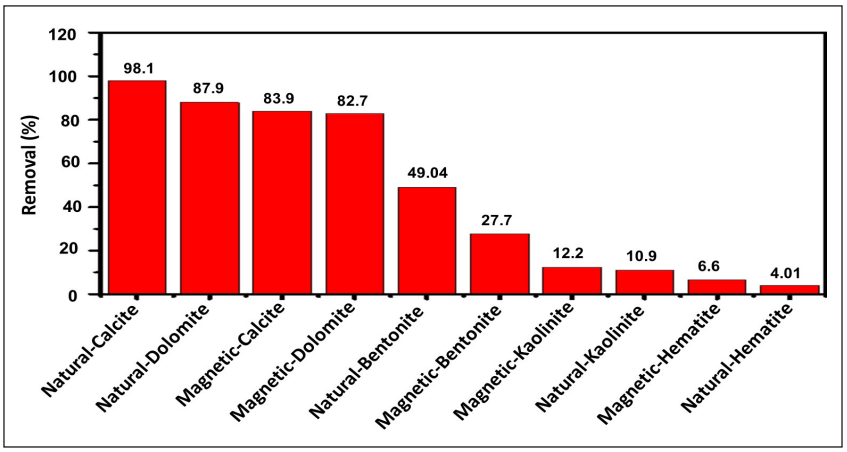

Figure 1. Comparison of the As(III) adsorption efficiencies of various adsorbents

Table 1. Chemical composition of the selected natural calcite adsorbent (% by weight)

Sample	Cao	SiO_2	Na_2O	Al_2O_3	MgO	K_2O	Fe_2O_3	L.O.I
Calcite	45.7	18.0	3.0	1.23	1.0	0.27	0.20	30.0

L.O.I: loss on ignition

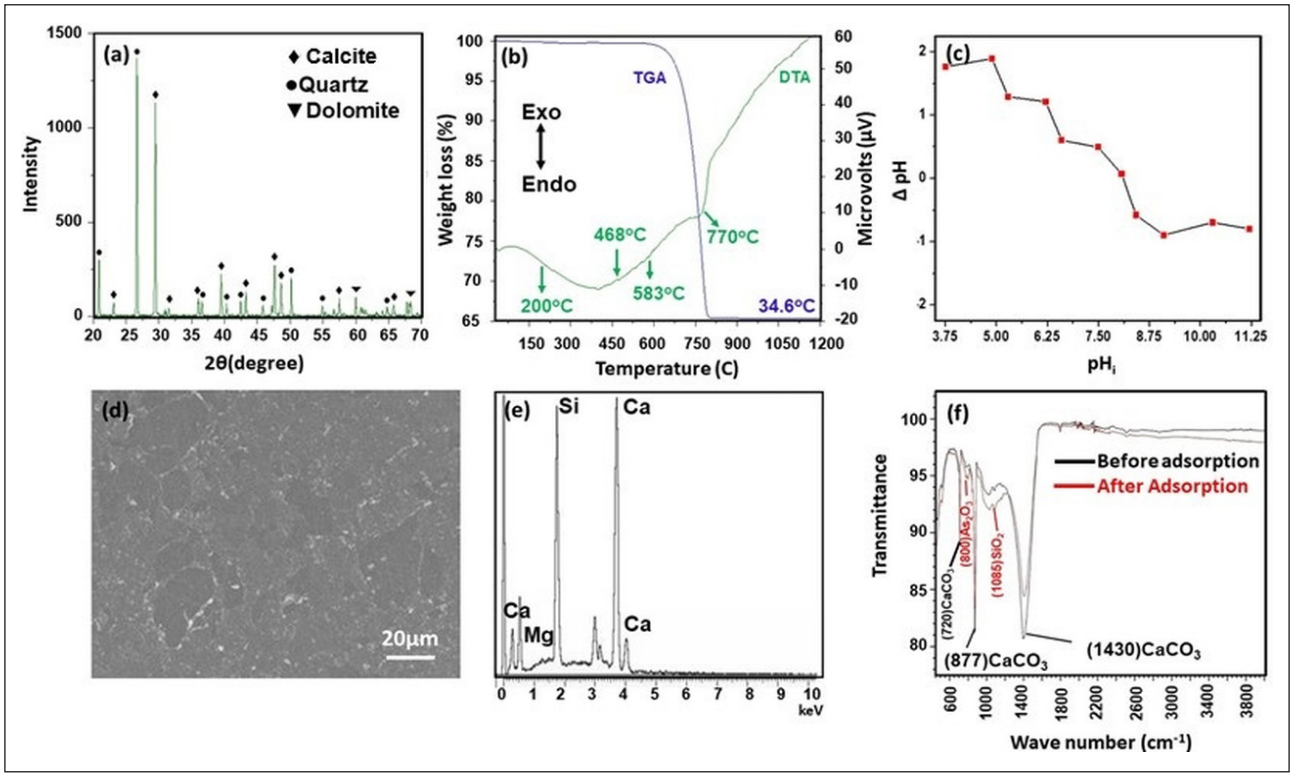

Figure 2. Structural characterizations: (a) XRD pattern of the calcite sample (b) TG/DTA plot for the calcite, (c) PZC plot for calcite at 298 K, (d) secondary electron SEM image, (e) EDS spectrum for calcite, and (f) FT-IR spectra of calcite before and after As(III) adsorption

In the DTA curve, the only exothermic peak observed was at 468°C, associated with pyrite oxidation. A small endothermic dip observed at 583°C was due to the conversion of α-quartz to ß-quartz, confirming the XRF results which detected silica in substantial amounts. Furthermore, the clearly resolved endothermic peak on the DTA curve at the decomposition temperature confirm the crystallinity of the carbonate phase, agreeing well with the XRD result.

Point of zero charge

The magnitude of the point of zero charge (pH_{PZC}) is helpful to predict the electrical charge produced on the surface due to the phenomena of protonation and deprotonation of the adsorbent. It is the pH at which the net surface charges on the adsorbent surface is zero. When pH values become greater than pH_{PZC} then the surface gains negative charge and cations are selectively adsorbed. However, when pH values become lower than pH_{PZC}, the surface attains a positive charge and anions are specifically adsorbed (Shah et al., 2019). The pH_{PZC} of calcite was determined to be pH 8 (Fig. 2c). A similar pH_{PZC} value was also reported for bentonite clay adsorbent in our previous publication (Shah et al., 2018).

SEM-EDS analysis

The SEM in conjunction with the EDS spectrum was used for studying the surface morphology and for elemental analysis of the calcite adsorbent. The structure observed under SEM is moderately smooth and flat (Fig. 2d). The EDS spectrum recorded on the surface of the sample showed the presence of calcium (Ca), silica (Si) and magnesium (Mg) in varying amounts (Fig. 2e). The EDS data showed the percentage composition of calcium as 63%, silicon as 33% and magnesium as ~1% by weight, which was consistent with the XRF and XRD results. The prominent silver (Ag) peak that appeared in the EDS spectrum is because the sample was silver coated in order to avoid it becoming charged priorto SEM analysis.

FTIR analysis

The results for FT-IR analysis before and after adsorption of As(III) onto calcite are presented in Fig. 2f. The characteristic FT-IR peaks of calcite (black) at 1 430 cm^{-1} correspond to asymmetric stretching vibrations, whereas the peaks at 877 and 720 cm^{-1} are associated with the asymmetric and symmetric bending vibrations of carbonate groups (CO_3^{2-}), respectively (Dabbas et al., 2014; Gunasekaran et al., 2006). After As(III) adsorption on calcite, the peak intensities at 1 430, 877 and 720 cm^{-1} clearly decreased, indicating the interaction of As(III) with carbonates in calcite. In addition, a new band at 800 cm^{-1} appeared after adsorption, which indicates the stretching vibration of As–O, confirming the adsorption of As(III) on calcite (Miller and Wilkins, 1952; Huang et al., 2017). The IR results in the current investigations agree well with the previous results reported in literature (Zuo et al., 2017). Moreover, other IR peaks did not change remarkably after As(III) adsorption, which implies that the adsorption process was mainly controlled by CO_3^{2-} sites at the calcite surface.

Effect of contact time and temperature

Kinetic experiments were performed to study the effect of contact time on As(III) removal by calcite at four different temperatures (Fig. 3a). It is clear from Fig. 3a that the rate of As(III) removal by calcite increases with increasing temperature and time, verifying the significant effect of temperature and time on the adsorption process. Furthermore, the adsorption of As(III) gradually and steadily increases up to 160 min (equilibrium time), with maximum uptake of 98%. After attainment of equilibrium, the availability of vacant active sites on the adsorbent surface is exhausted and no further increase in the uptake of As(III) happens. Thus, 160 min was selected as an optimum reaction time required for successful adsorption. It is clear from Fig. 3a that temperature has a profound effect on the uptake of As(III) ions and the per cent removal of As(III) was increased from 84.2 to 98.1% by increasing the temperature from 298 to 333K,

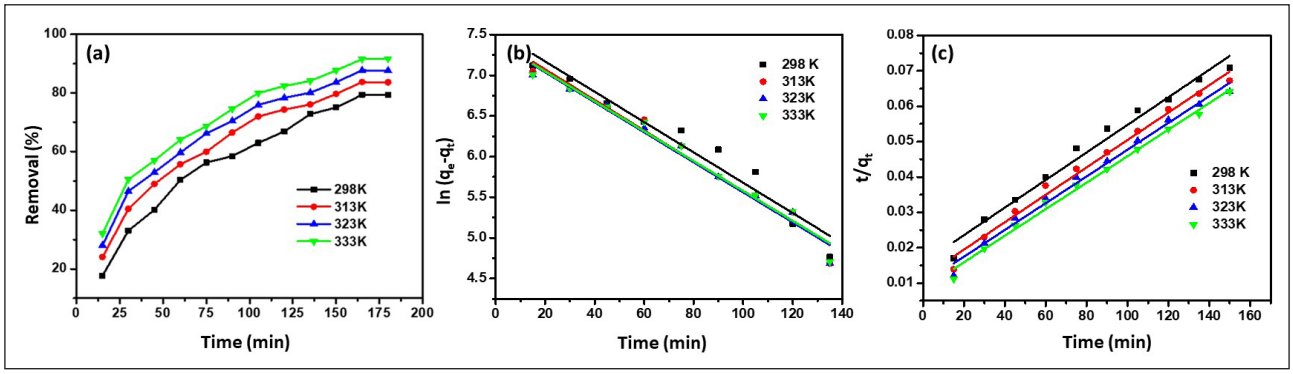

Figure 3. Kinetic studies of the adsorption of As(III) on natural and magnetically modified clays: (a) effect of contact time (b) pseudo-first-order plots and (c) pseudo-second-order plots for As(III)

Table 2. Pseudo-first and pseudo-second-order parameters for As(III) adsorption on calcite

Temp (K)	C_0 (µg·L^{-1})	$q_{e(exp)}$ (µg·g^{-1})	Pseudo-first-order			Pseudo-second-order		
			K_1 (min^{-1})	$q_{e(cal)}$ (µg·g^{-1})	R^2	K^2 (min^{-1})	$q_{e(cal)}$ (µg·g^{-1})	R^2
298	1 000	2 117.33	0.0181	1 798.87	0.9612	55 x 10^{-5}	2 164.50	0.9802
313	1 000	2 232.00	0.0185	1 671.09	0.9774	50 x 10^{-5}	2 398.08	0.9886
323	1 000	2 338.67	0.0183	1 625.57	0.9781	45 x 10^{-5}	2 352.94	0.9901
333	1 000	2 448	0.0182	3 061.96	0.9768	41 x 10^{-5}	2 457.00	0.9938

respectively, suggesting the endothermic nature of adsorption; however, the equilibrium time (160 min) remained independent of temperature during adsorption of As(III) on calcite.

Application of kinetic models

The pseudo-first-order and pseudo-second-order kinetic models were used to explain the kinetic data, which can be expressed in linear form as follows:

$$\ln\left(q_e - q_t\right) = \ln q_e - k_1 t \quad (3)$$

$$\frac{t}{q_t} = \frac{1}{k_2 q_e^{\,2}} + \frac{t}{q_e} \quad (4)$$

where k_1 and k_2 are pseudo-first and pseudo-second-order rate constants (min^{-1}) and (g·µg^{-1}·min) respectively, q_t and q_e (µg·g^{-1}) are the amount of As(III) ions adsorbed per unit time of adsorbent at time t and equilibrium, respectively. The pseudo first- and second-order plots are shown separately in Fig. 3b and Fig. 3c, indicating that the pseudo-second-order model could be better fitted to the kinetic data of As(III) adsorption compared to the pseudo-first-order model, as also shown in Table 2. This indicates an advantage of the pseudo-second-order model over the pseudo-first-order model for better explanation and evaluation of the kinetic data.

Effect of pH and adsorbent dosage

The effect of initial pH of As(III) solution on adsorption is shown in Fig. 4a. It is obvious that the rate of As(III) removal ions increased with the increase in pH from 2 to 7, and a maximum removal efficiency of 98% was observed. However, the per cent removal for As(III) was slightly decreased to 90.84, 90.81 and 90.76% at pH 8, 9 and 10, respectively. The difference in removal efficiency verses pH of solution can be justified on the basis of the presence of various arsenite species and surface charge of the calcite adsorbent. At pH < 7, the predominant species of As(III) exists as neutrally charged H_3AsO_3, suggesting the presence of physical forces of attraction between H_3AsO_3 and surface of adsorbent. However, when pH rises from 2 to 7, some of the H_3AsO_3 species dissociate into $H_2AsO_3^-$ and $HAsO_3^{2-}$ anions and more adsorption can be expected because of increasing electrostatic force of attraction. The reduction in removal efficiency beyond pH 7 can be due to the creation of repulsive forces between the negatively charged surface of the adsorbent and arsenite species. Another reason for decreasing adsorption may be the competition between OH^- ions and arsenite anions ($H_2AsO_3^-$ and $HAsO_3^{2-}$) for the same binding sites on the adsorbent surface (Uluozlu et al., 2008; Mahmood et al., 2018). Given these results, it can be suggested that natural calcite adsorbent can be a promising candidate for As(III) removal from contaminated natural water without any pH adjustment in the pH range 6–7.

Figure 4b depicts the effect of adsorbent dose on the removal of As(III). It can be noted from the figure that percentage removal increases by increasing adsorbent dose from 5 to 20 mg which is due to the increasing accessibility of available active vacant sites on the adsorbent surface for As(III) ion adsorption. Considering the trade-off between high adsorption efficiency and dosage amount, 20 mg of adsorbent was considered as the optimal dosage to use in succeeding adsorption experiments.

Effect of concentration and temperature

The equilibrium adsorption capacities of adsorbent calcite as a function of As(III) ion concentration and temperature are presented in Fig. 5a. The adsorption isotherm obtained matches the linear isotherm type, according to Giles classification for adsorption isotherms (Shah et al., 2019). The equilibrium adsorption capacity of the adsorbent was increased with increasing initial concentration and temperature of the media, indicating the endothermic nature of adsorption. An explanation for this behavior is proposed as the increase in the arsenite concentration and temperature in aqueous phase leading to increasing mass transfer driving forces and effective collisions between adsorbate and adsorbent, leading to an increase in As(III) adsorption capacity (Alshameria et al., 2018). Eventually, the maximum adsorption capacity (19.05 mg·g^{-1}) was obtained at the highest temperature (333K).

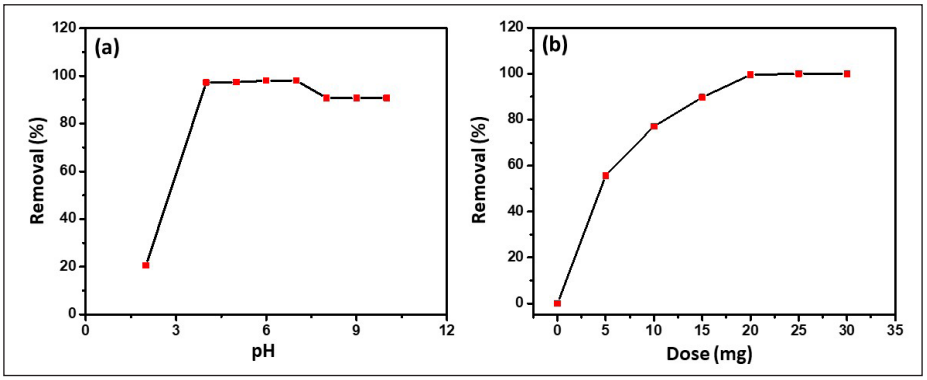

Figure 4. Adsorption studies: (a) effect pf pH, and (b) effect of adsorbent dose

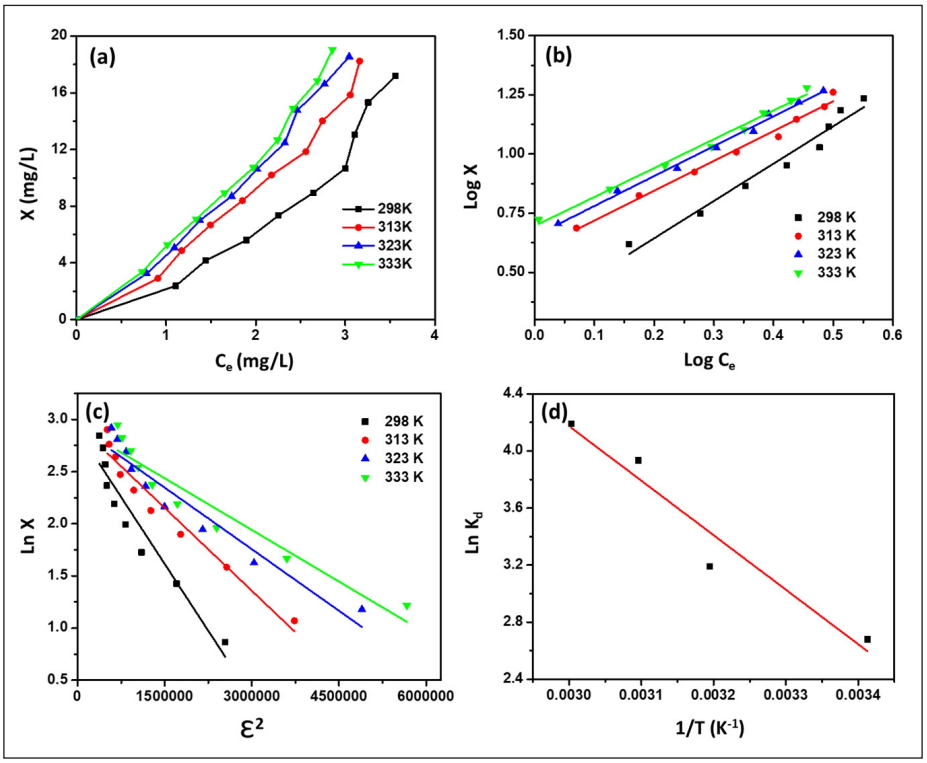

Figure 5. Adsorption isotherms: (a) Effect of temperature (b) Freundlich plots, (c) D-R plots and (d) thermodynamic plots for As(III) removal onto calcite

Application of adsorption models

The equilibrium data for As(III) adsorption by calcite was evaluated by Langmuir (LM), Freundlich (FM) and Dubinin-Radushkevich (D-R) models. LM, which describes the adsorption at a homogeneous surface of the adsorbent and assumes successfull monolayer adsorption, can be written as:

$$\frac{C_e}{X} = \frac{C_e}{X_m} + \frac{1}{K_b X_m} \tag{5}$$

where X_m (mg·g^{-1}) is the maximum adsorption capacity of adsorbent and K_b (L·mg^{-1}) is the binding energy constant, indicating binding forces responsible for the adsorption of adsorbate on adsorbent. The Freundlich adsorption isotherm assumes the heterogeneity of the surface with adsorption sites of different energy. The linear form of FM can be written as:

$$\ln X = \ln K_f + \frac{1}{n} \ln C_e \tag{6}$$

where C_e (mg·L^{-1}) is the equilibrium concentration and X (mg·g^{-1}) is the amount of As(III) adsorbed per unit mass of the adsorbent. K_f (mg·g^{-1}) and $1/n$ (L·mg^{-1}) are the Freundlich constants reflecting the saturation capacity of the adsorbent and intensity or strength of adsorption, respectively. Compared to LM, FM showed well-fitted adsorption data with high R^2 values, as shown in Fig. 5b. If $1/n = 1$ and n = 1–10, the adsorption isotherm is linear and adsorption is favourable, respectively. In the present study, the value of $1/n$ ranges from 0.625 to 0.705, while n ranges from 1.4 to 1.6, indicating that the adsorption of As(III) onto calcite is favourable (Table 3). The D-R isotherm model can be used as an approach to distinguish between the physical and chemical nature of adsorption processes. The linear form of this model is given below:

$$\ln X = \ln X_m - \beta\varepsilon^2 \tag{7}$$

where β (mol^2 ·J^{-2}) is a D-R constant associated with the mean adsorption energy E (kJ·mol^{-1}), which is defined as the amount of energy required for transferring 1 mole of adsorbate from infinity to the surface of the adsorbent, and ε is the Polanyi adsorption potential which can be calculated from the following equation:

$$\varepsilon = RT \ln(1 + \frac{1}{C_e}) \tag{8}$$

where R is the general gas constant (J·k^{-1}·mol^{-1}) and T is absolute temperature (K). The linear plots (ln X vs. ε^2) show a good fit of the D-R model, with high R^2 values, as shown in Fig. 5c. The mean adsorption energy (E), which is related to β, was calculated using the following relationship:

$$E = \frac{1}{(2\beta)^{\frac{1}{2}}} \quad (9)$$

The magnitude of E was used to determine whether the adsorption is physisorption or chemisorption. Generally, when the value of E is less than 8 kJ·mol^{-1} the adsorption is physical, if E = 8–16 kJ·mol^{-1} then adsorption takes place by ion exchange, whereas if E is higher than 16 kJ·mol^{-1} then chemical adsorption occurs (Shah et al., 2018). In the current investigation, the values of E were observed to be in the range of 0.765–0.815 kJ·mol^{-1}, suggesting that physical or weak electrostatic forces are involved in adsorption of As(III) on calcite, and that adsorption occurred via the outer sphere complexation mechanism (Table 3). Similar results were also reported elsewhere for the adsorption of Co(II) and Cr(VI) on calcium carbonate (Correa et al., 2013).

Thermodynamic studies

Using the temperature-dependent K_c values, thermodynamic parameters of enthalpy (ΔH) and entropy changes (ΔS) for the adsorption process were evaluated using the Von't Hoff equation:

$$\ln K_c = \frac{\Delta H}{RT} - \frac{\Delta S}{R} \quad (10)$$

where R is the gas constant (8.314 J·K^{-1}·mol^{-1}), T is absolute temperature (K) and K_c is the equilibrium constant which can be calculated using the following equation:

$$K_c = \frac{X}{C_e} \quad (11)$$

The Von't Hoff plots are represented in Fig. 5d, and the values of ΔH and ΔS were calculated from slope and intercept of ln K_c vs $1/T$ curves, respectively. The change in Gibbs free energy (ΔG) was determined using the following equation:

$$\Delta G = \Delta H - T\Delta S \quad (12)$$

The calculated thermodynamic parameters for adsorption of As(III) onto calcite are given in Table 4. The positive value of ΔH reflects the endothermic nature of the adsorption process, and that of ΔS indicates the increasing randomness or disorder of the solid/solution interface during adsorption.

Economic evaluation of calcite

The results of the current study were compared with those of previous studies (Table 4). It can be seen from the table that As(III) adsorption capacity of natural calcite was higher than for many other clay and rock-based adsorbents previously explored in literature (Chakravarty et al., 2002; Thirunavukkarasu et al., 2003; Gupta et al., 2005; Maji et al., 2008; Thao et al., 2008; Tian et al., 2011; Shin et al., 2014; Salameh et al., 2015; Huang et al., 2017; Shah et al., 2019; Nguyen et al., 2019). Also, it can be noted from the table that calcite was not chemically modified to improve the adsorption capacity, suggesting its potential for large-scale application in adsorption technology. Thus, it can be concluded that natural calcite is a potential eco-friendly and economic adsorbent with reasonable adsorption capacity and simple application for the treatment of wastewater and As(III) contaminated solutions.

Table 3. Freundlich adsorption parameters for As(III) adsorption on calcite

Temp. (*K*)	K_f (mg·g^{-1})	1/*n* (L·mg^{-1})	R^2
298	1.3703	0.621	0.980
313	1.5109	0.674	0.985
323	1.5680	0.694	0.987
333	1.5954	0.705	0.985

Table 4. Thermodynamic parameters for As(III) adsorption on calcite

Temp. (K)	Δ*G* (kJ·mol^{-1})	Δ*H* (kJ·mol^{-1})	Δ*S* (J·K^{-1}·mol^{-1})
293	−6.96	31.76	129.95
313	−8.91		
323	−10.21		
333	−11.51		

Table 5. Comparison of values of maximum adsorption capacities of calcite with published data on As(III) adsorption

Adsorbent	pH	Concentration	Maximum adsorption capacity (mg·g^{-1})	Reference
Calcite	6.8	2–10 (mg·L^{-1})	19.05	This work
Manganese ore	7	0.5–40 (mg·L^{-1})	18.52	Huang et al., 2017
Ferruginous Manganese ore	6.3		0.54	Chakravarty et al., 2002
Dolomite	8	2–10 (mg·L^{-1})	11.57	Shah et al., 2019
Charred dolomite	7.2	50–200 (µg·L^{-1})	1.846	Salameh et al., 2015
Laterite	-	-	0.17	Tian et al., 2011
Laterite	5	2–50 (mg·L^{-11})	0.756	Thao et al., 2008
Laterite soil	7.2	0–0.33 (mg·L^{-1})	1.384	Maji et al., 2008
Ban Cuon iron-ore sludge	5.5	0–50 (mg·L^{-1})	1.113	Nguyen et al., 2019
Red mud	7.25	33.37–400 (µg·L^{-1})	0.663	Shin et al., 2014
Red mud	7	0–50 (mg·L^{-1})	2.62	
Gibbsite	5.5	10–1 000 (mg·L^{-1})	3.30	Shin et al., 2014
Zeolite	7	0–50 (mg·L^{-1})	0.481	Shin et al., 2014
Lime-stone	7	0–50 (mg·L^{-1})	0.461	Shin et al., 2014
Iron oxide coated sand	7.5	100–800 (µg·L^{-1})	0.029	Thirunavukkarasu et al., 2003
Iron oxide coated sand	7.6	100 (µg·L^{-1})	0.041	Gupta et al., 2005

CONCLUSIONS

From the above discussion, it is suggested that calcite of KPK region of Pakistan can be considered as an ideal adsorbent for As(III) removal from water, due to its low cost, wide availability, and impressive removal efficiency. Calcite showed tremendous adsorption capability of 98% in the pH range from 4–7, which can make it useful adsorbent for practical application in natural water systems (pH 7) containing As(III) traces without any adjustment of pH. The comparison of current and previously published data showed good maximum adsorption capacity of our adsorbent (19.05 $mg{\cdot}g^{-1}$) as compared to reported values in the literature (Table 5). The adsorption data followed Freundlich and pseudo-second-order models, respectively. The results also proved that the adsorption process is thermodynamically feasible, spontaneous, endothermic, and physical in nature. FTIR confirmed the adsorption of As(III) on the surface of calcite was due to interaction of As(III) ions with CO_3^{2-}. Given the fact that natural calcite requires no pretreatment, it is an economic and green adsorbent with a satisfying adsorption capacity and could be employed effectively for the removal of As(III) at pilot and domestic scale.

ACKNOWLEDGMENTS

The research was supported by Higher Education Commission (HEC) of Pakistan through National Research Program for Universities (NRPU) Project No. 8817.

REFERENCES

ALSHAMERIA A, HE H, ZHUA J, XI Y, ZHUA R, MA L and TAO Q (2018) Adsorption of ammonium by different natural clay minerals, characterization, kinetics, and adsorption isotherms. *Appl. Clay Sci.* **159** 83–93. https://doi.org/10.1016/j.clay.2017.11.007

AMER MW and AWWAD AM (2018) Removal of As(V) from aqueous solution by adsorption onto nanocrystalline kaolinite: Equilibrium and thermodynamic aspects of adsorption. *Environ. Nanotechnol. Monit. Manag.* **9** 37–41. https://doi.org/10.1016/j.enmm.2017.12.001

ANNEERSELVAM P, MORAD N and TAN KA (2011) Magnetic nanoparticle (Fe_3O_4) impregnated onto tea waste for the removal of nickel (II) from aqueous solution. *J. Hazardous Mater.* **186** 160–168. https://doi.org/10.1016/j.jhazmat.2010.10.102

AREDES S, KLEIN B and PAWLIK M (2012) The removal of arsenic from water using natural iron oxide minerals. *J. Clean. Prod.* **29–30** 208–213. https://doi.org/10.1016/j.jclepro.2012.01.029

CHAKRAVARTY S, DUREJA V, BHATTACHARYYA G, MAITY S and BHATTACHARYYA S (2002) Removal of arsenic from groundwater using low-cost ferruginous manganese ore. *Water Res.* **36** 625–632. https://doi.org/10.1016/S0043-1354(01)00234-2

CHERIAN T and NARAYANA B (2005) A new spectrophotometric method for the determination of arsenic in environmental and biological samples. *Anal. Lett.* **38** 2207–2216. https://doi.org/10.1080/00032710500260555

CORREA FJ, ALCANTARA EG and BECERRIL JJ (2013) Study of Co (II) and Cr (VI) dsaorption from aqueous solution by $CaCO_3$. *J. Chem. Soc. Pakistan* **35** 1088–1095.

DABBAS MA, EISA MY and KADHIM WH (2014) Estimation of gypsum-calcite percentages using a Fourier transform infrared spectrophotometer (FTIR), in Alexandria gypsiferous soil – Iraq. *J. Raman Spectrosc.* **55** 1916–1926.

FAHAD M and IQBAL Y (2014) Kinetic and thermodynamic study of calcite marble samples from lesser Himalayas. *Int. J. Thermophys.* **35** 361–374. https://doi.org/10.1007/s10765-014-1601-9

FAHAD M, IQBAL Y, RIAZ M, UBIC R and REDFERN SAT (2016) Metamorphic temperature investigation of coexisting calcite and dolomite marble examples from Nikani Ghar marble and Nowshera Formation, Peshawar Basin, Pakistan. *J. Earth Sci.* **27** 989–997. https://doi.org/10.1007/s12583-015-0643-7

FAHAD M and SUNDAS S (2018) Determination and estimation of magnesium content in the single-phase magnesium-calcite [Ca(1–x) MgxCa(s)] using electron probe micro analysis (EPMA) and x-ray diffraction (XRD). *Geosci. J.* **22** 303–312. https://doi.org/10.1007/s12303-017-0059-8

GAN F, XI H, HUANG Q and DENG Y (2019) Assessing and modifying China bentonites for aflatoxin adsorption. *Appl. Clay Sci.* **168** 348–354. https://doi.org/10.1016/j.clay.2018.12.001

GUNASEKARAN S, ANBALAGAN G and PANDI S (2006) Raman and infrared spectra of carbonates of calcite structure. *J. Raman Spectrosc.* **37** 892–899. https://doi.org/10.1002/jrs.1518

GUPTA VK, SAINI VK and NEERAJ J (2005) Adsorption of As(III) from aqueous solutions by iron oxide-coated sand. *J. Colloid Interf. Sci.* **288** 55–60. https://doi.org/10.1016/j.jcis.2005.02.054

JEON E, RYU S, PARK S, WANG L, TSANG DCW and BAEK K (2018) Enhanced adsorption of arsenic onto alum sludge modified by calcinations. *J. Clean. Prod.* **176** 54–62. https://doi.org/10.1016/j.jclepro.2017.12.153

HAO L, WANQ N, WANQ C and LI G (2018) Arsenic removal from water and river water by the combined adsorption–UF membrane process. *Chemosphere.* **202** 768–776. https://doi.org/10.1016/j.chemosphere.2018.03.159

HERNANDEZ-FLORES H, PARIONA N, HERRERA-TREJO M, HDZ-GARICA HM and MTZ-ENRIQUEZ AI (2018) Concrete/maghemite nanocomposites as novel adsorbents for arsenic removal. *J. Mol. Struct.* **1171** 9–16. https://doi.org/10.1016/j.molstruc.2018.05.078

HUANG Y, NIU C, QIU Q, XU W, GAO H, SHE R and TU S (2017) Study on the removal performance of natural manganese ore and iron-oxidizing bacteria on the arsenic. *J. Residual Sci. Technol.* **14** 379–386.

LIN C, LUO W, LUO T, ZHOU Q, LI H and JING L (2018) A study on adsorption of Cr (VI) by modified rice straw: Characteristics, performances, and mechanism. *J. Clean. Prod.* **196** 626–634. https://doi.org/10.1016/j.jclepro.2018.05.279

LIU CH, CHUANG YH, CHEN TY, TIAN Y, LI H, WANG MK and ZHANG W (2015) Mechanism of arsenic adsorption on magnetite nanoparticles from water: thermodynamic and spectroscopic studies, *Environ. Sci. Technol.* **49** 7726–7734. https://doi.org/10.1021/acs.est.5b00381

MAJI SK, PAL A and PAL T (2008) Arsenic removal from real-life groundwater by adsorption on laterite soil. *J. Hazardous Mater.* **151** 811–820. https://doi.org/10.1016/j.jhazmat.2007.06.060

MAHMOOD T, ASLAM M, NAEEM A, SIDDIQUE T and DIN SU (2018) Adsorption Of As(III) from aqueous solution onto iron impregnated used tea activated carbon: equilibrium, kinetic and thermodynamic study. *J. Chil. Chem. Soc.* **63** 3855–3866. https://doi.org/10.4067/s0717-97072018000103855

MILLER FA and WILKINS CH (1952) Infrared spectra and characteristic frequencies of inorganic ions. *Anal. Chem.* **24** 1253–1294. https://doi.org/10.1021/ac60068a007

MOMINA, SHAHDAT M and ISAMIL S (2018) Regeneration performance of clay-based adsorbents for the removal of industrial dyes: a review. *RSC Adv.* **8** 24571–24587. https://doi.org/10.1039/C8RA04290J

NGUYEN KM, NGUYEN BQ, NGUYEN HT and NGUYEN HTH (2019) Adsorption of arsenic and heavy metals from solutions by unmodified iron-ore sludge. *Appl. Sci.* **9** (4) 619. https://doi.org/10.3390/app9040619

RAMOS MAV, YAN W, LI X, KOEL BE and ZHANG W (2009) Simultaneous oxidation and reduction of arsenic by zero-valent iron nanoparticles: Understanding the significance of the core-shell structure. *J. Phys. Chem. C.* **113** 14591–14594. https://doi.org/10.1021/jp9051837

SALAMEH Y, ALBADARIN AB, ALLEN S, WALKER G and AHMAD MNM (2015) Arsenic(III,V) adsorption onto charred dolomite: Charring optimization and batch studies. *Chem. Eng. J.* **259** 663–671. https://doi.org/10.1016/j.cej.2014.08.038

SANJRANI MA, MEK T, SANJRANI ND, LEGHARI SJ, MORYANI HT and SHABNAM AB (2017) Current situation of aqueous arsenic contamination in Pakistan, focused on Sindh and Punjab Province, Pakistan: a review. *J. Pollution Effects Control.* **5** 1–8.

SARDI S, JOHNSON BB, RUYTER-HOOLEY M and ANGOVE MJ (2018) The adsorption of nortriptyline on montmorillonite, kaolinite, and gibbsite. *Appl. Clay Sci.* **165** 64–70. https://doi.org/10.1016/j.clay.2018.08.005

SHAH KH, ALI S, SHAH F, WASEEM M, ISMAIL B, KHAN RA, KHAN AM and KHAN AR (2018) Magnetic oxide nanoparticles (Fe_3O_4) impregnated bentonite clay as a potential adsorbent for Cr (III) adsorption. *Mater. Res. Express*. **5** 096102. https://doi.org/10.1088/2053-1591/aad50e

SHAH KH, AYUB M, FAHAD M, BILAL M, ZZFAR BA and HUSSAIN Z (2019) Natural dolomite as a low-cost adsorbent for efficient removal of As(III) from aqueous solutions. *Mater. Res. Express*. **6** 085535. https://doi.org/10.1088/2053-1591/ab24f8

SIDDIQUI SI and CHAUDHRY SA (2017) Iron oxide and its modified forms as an adsorbent for arsenic removal: a comprehensive recent advancement. *Process Saf. Environ. Prot*. **111** 592–626. https://doi.org/10.1016/j.psep.2017.08.009

THAO NPH, HA NTH and ANH BTK (2016) Sorption of heavy metals by laterite from Vinh Phuc and Hanoi. Vietnam. *J. Viet. Environ*. **8** 235–239. https://doi.org/10.13141/jve.vol8.no4.pp235-239

THIRUNAVUKKARASU OS, VIRARAGHAVAN T and SUBRAMANIAN KS (2003) Arsenic removal from drinking water using iron coated sand. *Water Air Soil Pollut*. **142** (1) 95–111. https://doi.org/10.1023/A:1022073721853

TIAN Y, WU M, LIN HP and HUANQ Y (2011) Synthesis of magnetic wheat straw for arsenic adsorption. *J. Hazardous Mater*. **193** 10–16. https://doi.org/10.1016/j.jhazmat.2011.04.093

ULUOZLU OD, SARI A, TUZEN M and SOYLAK M (2008) Biosorption of Pb (II) and Cr (III) from aqueous solution by lichen (Parmelina tiliaceae) biomass. *Bioresour. Technol*. **99** 2972–2980. https://doi.org/10.1016/j.biortech.2007.06.052

VILARDI G, PALMA LD and VERDONE N (2018) Heavy metals adsorption by banana peels micro-powder: Equilibrium modeling by non-linear models. *Chin. J. Chem. Eng*. **26** 455–464. https://doi.org/10.1016/j.cjche.2017.06.026

SHIN WS, KANG KU and KIM YK (2014) Adsorption characteristics of multi-metal ions by red mud, zeolite, limestone, and oyster shell. *Environ. Eng. Res*. **19** (1) 15–22. https://doi.org/10.4491/eer.2014.19.1.015

YU Y, YU L, SHIN K and CHEN JP (2018) Yttrium-doped iron oxide magnetic adsorbent for enhancement in arsenic removal and ease in separation after applications. *J. Colloid Interf. Sci*. **521** 252–260. https://doi.org/10.1016/j.jcis.2018.02.046

ZUO WQ, CHEN C, CUI HJ and FU ML (2017) Enhanced removal of Cd (II) from aqueous solution using $CaCO_3$ nanoparticle modified sewage sludge biochar. *RSC Adv*. **7** 16238–16243. https://doi.org/10.1039/C7RA00324B